Journal of Innovative Optical Health Sciences
Vol. 8, No. 5 (2015) 1550010 (20 pages)

DOI: 10.1142/S1793545815500108

Analysis of entropies based on empirical mode decomposition in amnesic mild cognitive impairment of diabetes mellitus

Dong Cui*, Jinhuan Wang*, Zhijie Bian†, Qiuli Li‡,
Lei Wang‡ and Xiaoli Li†,§,¶,‖
*School of Information Science and Engineering
Yanshan University, Qinhuangdao, P. R. China
†School of Electrical Engineering
Yanshan University, Qinhuangdao, P. R. China
‡Department of Neurology
General Hospital of Second Artillery Corps of PLA
Beijing, P. R. China
§State Key Laboratory of Cognitive Neuroscience
and Learning & IDG/McGovern Institute for Brain Research
Beijing Normal University, Beijing, P. R. China
¶Center for Collaboration and Innovation
in Brain and Learning Sciences
Beijing Normal University, Beijing, P. R. China
‖xiaoli@bnu.edu.cn

Received 22 June 2014
Accepted 7 October 2014
Published 19 November 2014

EEG characteristics that correlate with the cognitive functions are important in detecting mild cognitive impairment (MCI) in T2DM. To investigate the complexity between aMCI group and age-matched non-aMCI control group in T2DM, six entropies combining empirical mode decomposition (EMD), including Approximate entropy (ApEn), Sample entropy (SaEn), Fuzzy entropy (FEn), Permutation entropy (PEn), Power spectrum entropy (PsEn) and Wavelet entropy (WEn) were used in the study. A feature extraction technique based on maximization of the area under the curve (AUC) and a support vector machine (SVM) were subsequently used to for features selection and classification. Finally, Pearson's linear correlation was employed to study associations between these entropies and cognitive functions. Compared to other entropies, FEn had a higher classification accuracy, sensitivity and specificity of 68%, 67.1% and 71.9%, respectively. Top 43 salient features achieved classification accuracy, sensitivity and specificity of

‖Corresponding author.

73.8%, 72.3% and 77.9%, respectively. P4, T4 and C4 were the highest ranking salient electrodes. Correlation analysis showed that FEn based on EMD was positively correlated to memory at electrodes F7, F8 and P4, and PsEn based on EMD was positively correlated to Montreal cognitive assessment (MoCA) and memory at electrode T4. In sum, FEn based on EMD in right-temporal and occipital regions may be more suitable for early diagnosis of the MCI with T2DM.

Keywords: Entropy; empirical mode decomposition; amnestic mild cognitive impairment; type 2 diabetes mellitus.

1. Introduction

Diabetes mellitus (DM) has a negative impact on the survival and quality of life in patients. It was estimated that about 90% of DM patients suffered from type 2 diabetes mellitus (T2DM). T2DM has become one of the most globally diffused pathologies in the world.[1] T2DM is associated with a variety of adverse complications, such as cardiovascular diseases, lung dysfunction and retinopathy, and has an increased risk of cognitive impairment and dementia.[2–5]

Mild cognitive impairment (MCI) has been described as a transitional state between normal cognition and Alzheimer's disease (AD) in clinical and research fields.[2] Some studies have indicated that DM was recognized as a risk factor for the development of probable AD[6] and the MCI, especially the amnestic mild cognitive impairment (aMCI).[7] Cukierman *et al.* indicated that people with DM have 1.5 times greater risk of cognitive decline, and 1.6 times greater risk of future dementia compared to people without DM.[8] Many quantitative measures, such as Fourier transform,[9,10] synchronization likelihood,[11] correlation dimension,[12] entropy,[13–17] coherence,[18] multiway array decomposition (MAD) analysis,[19] wavelet power spectral analysis[20] and amplitude modulation analysis[21] have been developed to quantify the changes of EEG in MCI and AD.

Due to the complex interconnections between neurons, the EEG signals are complex, nonlinear and nonstationary. The nonlinear EEG complexity analysis, such as entropy, can determine the probability of finding specific patterns in a time series and analyze the irregularity or predictability of a time series. Some entropy methods have been successfully applied to pathological development.[13–17,22,23] Abásolo *et al.* analyzed the regularity of nonlinear EEG background activity from 19 recording electrodes, and found that Approximate entropy (ApEn) and Sample entropy (SaEn) were significantly lower in the AD patients compared with healthy control subjects, which illustrated an increase in EEG regularity in AD patients.[17,24] Tsai *et al.* applied SaEn to evaluate the irregularity of the EEG signals of AD patients and demonstrated that the irregularity of EEG signals is reduced in demented patients.[14]

Although some research based on entropy have been used to study the DM in recent years, such as measurement of complexity of heart rate variability in T2DM,[25] assessment of atherosclerosis in the aged and DM[26] and assessment of muscle metabolic pattern in T2DM,[27] there are rarely any studies in the cognitive function of DM using entropy. Hazari *et al.* analyzed P300 amplitude in T2DM patients and nondiabetic controls, and found that P300 ERPs revealed cognitive dysfunction which was not detected by neuro-psychometric test (mini mental state evaluation — MMSE). Patients with T2DM have decreased cognitive function which is more prominent when the disease duration exceeds five years. Co-existence of hypertension with T2DM further increases the risk of cognitive impairment.[28] EEG on type 1 diabetes mellitus (T1DM) patients in resting position demonstrated a decline in the power of fast activity (alpha and beta band) in the posterior temporal regions, and an increase in slow spectral components in the frontal regions. T2DM demonstrated similarly.[29–31]

In this study, we used six entropy analysis measures for aMCI detection in T2DM. Before calculating the entropy, the EMD method was used to decompose EEG signals. EMD has become a useful tool for the decomposition and time-frequency analysis of nonstationary signals in recent years. Contrary to almost all the previous decomposing methods, EMD is empirical, intuitive, direct and adaptive in nature. In particular, the intrinsic mode functions (IMFs) produced by the EMD method usually have physical meanings.[32] The performance

of the six entropies was evaluated by a Logistic map simulation model. Then, the dynamic characteristics in T2DM were analyzed by a simple feature selection algorithm based on the area under the curve (AUC) maximization and the support vector machines (SVM). We want to explore which entropies and brain areas can assist in early clinical detection between aMCI and control groups in T2DM.

2. Materials and Methods

2.1. *Subjects and criteria*

We recruited 21 patients in T2DM (12 females, 9 males), whose diagnosis and classification criteria of DM were recommended by the World Health Organization.[33] The patients were from the Neurology Department of Second Artillery General Hospital of Beijing in China. Beijing Normal University ethics committee approved the study. Each participant provided voluntary informed consent before the experiment.

The T2DM subjects comprised of two groups. One group included 11 subjects (4 males, 7 females) as the aMCI group. The other group included 10 non-aMCI subjects (5 males, 5 females) matching with age and educational level as control group. Inclusion criteria for aMCI group in T2DM were (1) reporting of a decline in cognitive functioning relative to previous abilities during the past year by the patient or their families; (2) cognitive disorders as evidenced by clinical evaluation (with the hypomnesia of chief complaint, or in another cognitive domain, which in this study was assessed by neuropsychological test such as MMSE and Montreal cognitive assessment (MoCA); (3) the activity of daily living was unaffected as documented by history. The evidence of independent living was assessed by instrumental activity of daily living (IADL) Scale test.[34] To exclude other causes of reversible dementias or severe cognitive functions, exclusion criteria for aMCI group were (1) MCI group without objective memory deficits; (2) with any psychiatric or other neurological disorders such as AD, dementia, Parkinsonism, depression, extrapyramidal disease, brain trauma, brain tumor, epilepsy, neuropathic recession, etc.; (3) severe physical illness, such as the clinical macro-vascular complications (angina, history of myocardial infarction, cerebral infarction with clinical symptoms and peripheral vascular embolism, etc.); (4) other psychiatric diseases, epilepsy, drug addiction, alcohol dependence, and use of psychoactive drugs or other drugs enhancing brain cognitive functions.

Inclusion criteria of the control group in T2DM were (1) no memory impairment chief complaint and normal activities of daily living; (2) normal cognitive functions as evidenced and assessed by neuropsychological test such as MMSE and MoCA. Exclusion criteria were chronic systemic illnesses, and subjects with a history of present or previous neurological or psychiatric disease.

All participants underwent general demographic and neuropsychological assessments. They were assessed by the MMSE and the MoCA, and some tests were used to assess memory, language, activities of daily living, the executive function and attention in each participant. Immediate and delayed recall measure and the re-evoked measures of the rey auditory verbal learning test (rAVLT)[35] were used to assess memory. Semantic Fluency Test of the one minute verbal fluency for animals and Boston Naming Test[36] were used to assess the language. The Digit Span Test[37] and the Trail Making Test parts A and B[38] were used to assess executive function and attention. IADL scale[39] was used to assess the activities of daily living.

Independent samples from the t-test analysis were used to measure the difference between aMCI group and control group by SPSS20.0 (IBM SPSS, Inc., NY, Armonk, USA). Significant level was set at $p < 0.05$. The results are shown in Table 1. In demographic tests, there was no significant difference between the two groups. In neuropsychological tests, the MMSE score, Digit Span Test, IADL, Semantic Fluency Test, Track Makings and Boston naming test did not produce any significant difference between the two groups. However, aMCI group was significantly lower in MoCA score, the AVLT immediate recall, delayed recall and delay re-evoke compared with control group. That is to say, the performance of control group was better than aMCI group in the memory functions. There was no significant difference between the two groups in the executive function and attention, the activity of daily living and language.

2.2. *EEG recording and preprocessing*

EEG data were recorded in subjects in resting position with closed eyes from 128 electrodes with Cz as the reference electrode. Impedances were kept

Table 1. Demographic and neuropsychological characteristics in the aMCI group and control subjects. Significant level was set at $^*p < 0.05$, $^{**}p < 0.01$.

Factor	aMCI (Mean ± S.D.)	Control (Mean ± S.D.)	p-value
Total number	11	10	—
Male/Female	4/7	5/5	—
Age	71.55 ± 6.53	72.2 ± 6.97	NS
Educational level	13.73 ± 3.72	13.1 ± 2.51	NS
MMSE	27.91 ± 3.56	28.8 ± 0.42	0.429
MoCA	22.55 ± 1.21	27 ± 1.33	<0.000**
AVLT immediate recall	5.52 ± 0.89	8.09 ± 1.7	0.001*
AVLT delayed recall	3.36 ± 2.2	10 ± 2.16	<0.000**
AVLT delay re-evoke	10.82 ± 3.97	13.7 ± 1.42	0.043*
Trail making A	69.6 ± 20.6	61.2 ± 17.3	0.336
Trail making B	131.25 ± 64.89	108.1 ± 39.18	0.362
Boston naming test	19.45 ± 0.82	19.8 ± 0.42	0.238
Semantic Fluency Test	16.82 ± 3.16	18.36 ± 4.2	0.384
Digit Span Test	10.24 ± 2.41	14.8 ± 2.3	0.150
IADL	2.64 ± 4.32	0.5 ± 1.58	0.150

less than 50 kΩ. All data were recorded at 1000 Hz sample frequency with a range 0–200 Hz bandpass filter. The EEG epochs with ocular, muscular, and other types of artifacts were preliminarily eliminated visually by expert electroencephalographers. Then, consecutive EEG data of 18 channels (Fp1, Fp2, F7, F3, Fz, F4, F8, T3, C3, T4, T5, C4, P3, Pz, P4, T6, O1, O2) were divided into epochs of 5s for the follow-up analysis.

2.3. *Methods*

2.3.1. *Empirical mode decomposition*

EMD is a signal processing method, and has been more widely used in signal processing. EMD represents any temporal signal consisting of a finite set of amplitude and frequency modulated (AM-FM) oscillating components which are the basis of decomposition. The EMD can extract a linear combination of intrinsic oscillatory modes. The original signal $y(t)$ can be expressed as:

$$y(t) = \sum_{i=1}^{n} C_i + r_n, \tag{1}$$

where C_i represents the IMFs, n is the number of IMFs and r_n is the final residue.

Each IMF exhibited by the EMD captures the properties of the original signal at different time scales. Moreover, with a basis of decomposition based on the signal, it does not require a predefined basis for the signal. The more complex the signal is, the more random and uniform is the energy distribution, the more abundant is the frequency component, while the simpler the signal, the more concentrated is the energy distribution in a few energy modes. So the energy method is given by:

$$E_i = \frac{1}{N} \sum_{j=1}^{N} |C_i(j)|^2, \quad i = 1, 2, \ldots, n, \tag{2}$$

where E_i is the energy density of IMF C_i, and N is the length of original signal.

Each of these IMFs is composed of useful information or just composed of noise. High energy density of the IMF contains more main information of original signal and it accurately and effectively reflects signal characteristics, while low energy density of the IMF contains some information composed of noise. In this study, considering the noises and artifacts in EEG, the IMFs containing 90% feature energy density were selected and summed to reconstruct the signals, and entropy of the reconstructed signals was then calculated. The detailed EMD algorithm is described in Appendix A.

2.3.2. *ApEn based on EMD*

ApEn firstly proposed by Pincus,[40] has been widely applied in many fields, especially in complex and irregular biomedical signals, such as the EEG background activity of AD,[24] eplieptic activity[41] and heart rate signals.[42] Compared with Shannon's entropy, ApEn can express the randomness or

regularity of a time series in multiple dimensions. For the dominant analyzed series $x(i)$ of N length, ApEn is given by:

$$\mathrm{ApEn}(m,r,N) = \phi^m(r) - \phi^{m+1}(r), \tag{3}$$

where

$$\phi^m(r) = (N-m+1)^{-1} \sum_i \ln C_i^m(r), \tag{4}$$

$$C_i^m(r) = (N-m+1)^{-1} N_i^m(r), \quad i = 1, 2, \ldots, N-m+1, \tag{5}$$

where $C_i^m(r)$ is the probability of a vector $X(i)$ being similar to $X(j)$ within r, $N_i^m(r)$ is the number that the distance of two vectors $X(i)$ and $X(j)$ is smaller than the tolerance$r$, and a vector $X(i)(1 \le i \le N-m+1)$ is reconstituted of this series, and is expressed as $X(i)=\{x(i), x(i+1), \ldots, x(i+m-1)\}$.

Low value of ApEn means more regular time series, whereas high value of ApEn means more complexity and irregularity of the signal. The selection and the calculation of m and r are key problems. If the r values are smaller, one usually achieves poor conditional probability estimates. If the r values are large, much of the detailed information of the system is lost. Some studies have recommended to estimate ApEn with parameter values of $m = 2$–3, and $r = 0.1$–0.25 of the standard deviation of the signal.[43,44] In this study, we set $m = 2$, $r = 0.2$ of the standard deviation for the processed signal. The detailed algorithm is described in Appendix B.

2.3.3. *SaEn based on EMD*

SaEn is a modification of ApEn algorithm which avoids the bias caused by self-matching, and the improved performance of SaEn makes it useful for physiological signals.[45] It is largely independent of record length and displays relative consistencies under circumstances where ApEn does not. For the dominant analyzed series $x(i)$ of N length, SaEn excludes self-matching when counting $B^m(r)$ and $A^m(r)$ within a tolerance r. SaEn is given by the formula:

$$\mathrm{SaEn}(m,r,N) = -\ln[A^m(r)/B^m(r)], \tag{6}$$

where

$$A^m(r) = (N-m)^{-1} \sum_{i=1}^{N-m} C_i^{m+1}(r), \tag{7}$$

$$B^m(r) = (N-m)^{-1} \sum_{i=1}^{N-m} C_i^m(r), \tag{8}$$

$$C_i^m(r) = (N-m-1)^{-1} C_i, \quad i = 1, 2, \ldots, N-m, \tag{9}$$

where m is the embedding dimension, $B^m(r)$ is the probability that $X_m(i)$ and $X_m(j)$ will match for m points, $A^m(r)$ is the probability that $X_m(i)$ and $X_m(j)$ will match for $m+1$ points, $C_i^m(r)$ is the probability of a vector $X_m(i)$ being similar to $X_m(j)$ within r, C_i is the number that the distance of two vectors $X(i)$ and $X(j)$ is smaller than the tolerance r, and a vector $X_m(i)(1 \le i \le N-m+1)$ is reconstituted of this series, and is expressed as $X_m(i) = \{x(i), x(i+1), \ldots, x(i+m-1)\}$.

A lower value of SaEn also indicates more self-similarity in the time series. A higher value of SaEn also reflects more complexity or a less prediction in the time series. The same parameters with ApEn were used for the processed signal. The detailed algorithm is described in Appendix C.

2.3.4. *Fuzzy entropy based on EMD*

Fuzzy entropy (FEn) is based on fuzzy sets which was introduced by Zadeh,[46] and was employed to evaluate the information of pattern distribution in the pattern space. For the dominant analyzed series $x(i)$ of N length, FEn is given by:

$$\mathrm{FEn}(m,n,r,N) = \ln[\varphi^m(n,r) - \varphi^{m+1}(n,r)], \tag{10}$$

where

$$\varphi^m(n,r) = (N-m)^{-1} \sum_{i=1}^{N-m} \left[(N-m-1)^{-1} \sum_{j=1, j\neq i}^{N-m} D_{ij}^m \right], \tag{11}$$

$$\varphi^{m+1}(n,r) = (N-m)^{-1} \sum_{i=1}^{N-m} \left[(N-m-1)^{-1} \sum_{j=1, j\neq i}^{N-m} D_{ij}^{m+1} \right], \tag{12}$$

$$D_{ij}^m(n,r) = \mu(d_{ij}^m, n, r), \tag{13}$$

where X_i^m represents m consecutive x values, commencing with the ith points and generalized by removing a baseline: $u0(i) = m^{-1} \sum_{j=0}^{m-1} u(i+j)$, d_{ij}^m is the maximum absolute difference of the

corresponding scalar components of X_i^m and X_j^m, and D_{ij}^m is the similarity degree between X_i^m and its neighboring vector X_j^m through a fuzzy function $\mu(d_{ij}^m, n, r)$.

Parameters must be selected and determined before the calculation of FEn. A too large m value is unfavorable due to the need of a very large N (10^m–30^m), which is hard to meet generally and will lead to losing the information. As to the fuzzy similarity boundary determined by r and n, too narrow values will result in salient influence from noise, while too broad a boundary, as mentioned above, is supposed to be avoided for fear of information loss. In this study, m, r and n are fixed to 2, 0.2SD and 2, respectively. The detailed algorithm is described in Appendix D.

2.3.5. *Permutation entropy based on EMD*

Bandt and Pompe proposed the Permutation entropy (PEn) to measure the irregularity of nonstationary time series.[47] This method can quantify the complexity of a time-series comparing neighboring values to investigate the intrinsic structures in EEG data. The advantage of PEn has simplicity, robustness and easy computational complexity.[48] For the dominant analyzed series $x(i)$ of N length, the normalized PEn is defined as

$$H = -\frac{\sum_{i=1}^{n} p_i \log p_i}{\ln(n)}, \tag{14}$$

where n is possible order patterns, and p_i is the probability of the ith permutation occurring.

PEn gives a quantitative complexity measure for a dynamical time series. The smaller the value of PEn, the more regular the time series is. The calculation depends on the selection of m and L. If m is too small, there are only very few distinct states. If m is too large, it requires considerable long time sequence in order to make sure that every permutation patterns occurs. So it is necessary to investigate appropriate parameters for PEn calculation. Olofsen *et al.* suggested to estimate PEn with the embedding dimension values $m = 3$, and the time delay $L = 1$–2.[49] In this study, we calculated all EEG data with $m = 3$, $L = 1$. The detailed algorithm is described in Appendix E.

2.3.6. *Power spectrum entropy based on EMD*

Power spectrum entropy (PsEn) describes the irregularity of the signal spectrum. It is obtained by applying the Shannon entropy concept to the power distribution of the Fourier-transformed signal. For the dominant analyzed series $x(i)$ of N length, the PsEn is defined as

$$\mathrm{PsEn} = -\sum_{i=1}^{N} p_i \log p_i, \tag{15}$$

where p_i is the frequency of spectral amplitudes in bin i. The sum of all p_i is equal to 1.[50] The p_i can be obtained as the value of the power spectral density at each frequency bin.[51]

PsEn is an effective way to describe the degree of skewness in the frequency distribution. A high value of PsEn means a flat, uniform spectrum with a broad spectral content, whereas a low value of PsEn means a spectrum with all the power condensed into a single frequency bin.[52] In this study, the total spectral power was specified as the 0 to 80 Hz frequency band, and 2 Hz = 1 bin.

2.3.7. *Wavelet entropy based on EMD*

Wavelet entropy (WEn) can represent the degree of order/disorder of a multi-frequency signal, and provide useful information about the underlying dynamical process associated with the signal. For the dominant analyzed series $x(i)$ of N length, the WEn is defined between scales as

$$\mathrm{WEn} = -\sum_{j} p_j \log p_j, \tag{16}$$

where

$$p_j = \frac{E_j^{N_j}}{E_{\mathrm{tot}}} = \frac{\sum_k |C_j(k)|^2}{\sum_i \sum_k |C_j(k)|^2}, \tag{17}$$

where N_j is the window length within each level, and $C_j(k)$ are the wavelet coefficients of the local residual errors between successive signal approximations at scales j and $j+1$.

The WE is low when the signal represents an ordered activity characterized by a narrow frequency distribution, whereas the WE is high when the signal contains a broad spectrum of frequency distribution. The values of WEn are dependent on the wavelet basis function, the number of decomposed layers n and the data length N. In this study, the Daubechies6 (db6) wavelet was chosen as the wavelet basis function, where the number of decomposed layers was 6, the wavelet coefficients of

signals were in the range of 0–62.5 Hz bands. The detailed algorithm is described in Appendix F.

2.4. *Simulation model: Logistic map*

Logistic map is a well-known map arising in biology mathematics, and can exhibit chaotic dynamics. The logistic map is described by the following nonlinear polynomial equation:

$$x_{n+1} = ax_n(1 - x_n), \quad 0 \leq x_n \leq 1, \tag{18}$$

where x_n is a time series between zero and one which denotes the system state, and a is the system parameter.

Logistic map shows the different dynamics state when the parameter a is different, and a substantial change will occur in the dynamic state when the parameter a reaches a certain value. It presents a bifurcation diagram to the complexity and unpredictability of the chaotic process when the parameter a gradually increases from 3.5 to 4. In the study, the initial value x_0 was chosen to be 0.6, and the parameter a was from 3.5 to 4.

The maximal Lyapunov exponent was applied to analyze the dynamic predictability of logistic map systems, and it was defined as:

$$\lambda = \frac{1}{N}\sum_{n=1}^{N} \log_2|a(1 - 2x_n)|, \tag{19}$$

where a is the system parameter of logistic map, and N is the time series length in logistic map. The maximal negative Lyapunov exponent indicates stability, and maximal positive Lyapunov exponent indicates chaos. The bifurcation diagram of the logistic map and its maximal Lyapunov exponent are shown in Fig. 1. We could see that a substantial change had occurred in the dynamic state when the parameter a was at a certain value, for example, 3.832 was the negative maximum, and the complexities of time series achieved a minimum.

2.4.1. *The influence of noise and EMD on entropies algorithm*

The performance of six entropies to track dynamics state of logistic map and the influence of noise were evaluated by correlation analysis between the values of entropies and the largest positive Lyapunov exponent.

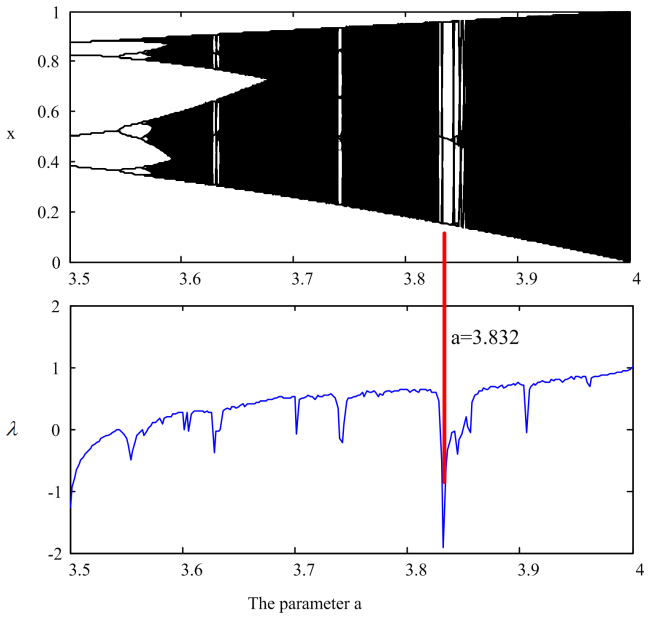

Fig. 1. Bifurcation diagram of the logistic map and its maximal Lyapunov exponent.

The values of the six entropies changed with system parameter a (from 3.5 to 4) with different signal-to-noise-ratio (SNR) (from 10 to 30 dB and original time series without noise) are shown in Fig. 2. The curves of six entropies based on EMD was similar, thus it was omitted. The correlation coefficients $r1$ (between each entropy and the maximal Lyapunov exponent) and $r2$ (between each entropy based on EMD and the maximal Lyapunov exponent) are shown in Table 2. The time series length N was 1000.

For original time series, all entropies could all track dynamics state of Logistic map well with correlation coefficients $r1$ up to 0.92, and they could effectively reflect the complexity and predictability of the chaotic series, except that PEn had a lower correlation coefficient $r1$ of 0.7904. When white noise was added to the system, the performance of tracking dynamics state of Logistic map in the six entropies all decreased, especially with small system parameter a. The correlation coefficients $r1$ of ApEn and SaEn declined rapidly with SNR 30 dB, but other entropies did not decline obviously. This indicates that the anti-noise performance of ApEn and SaEn was poorer than the others. The correlation coefficients $r1$ of FEn and PsEn were up to 0.92 with SNR 20 dB but not PEn and Wen which indicates that FEn and PsEn had better anti-noise

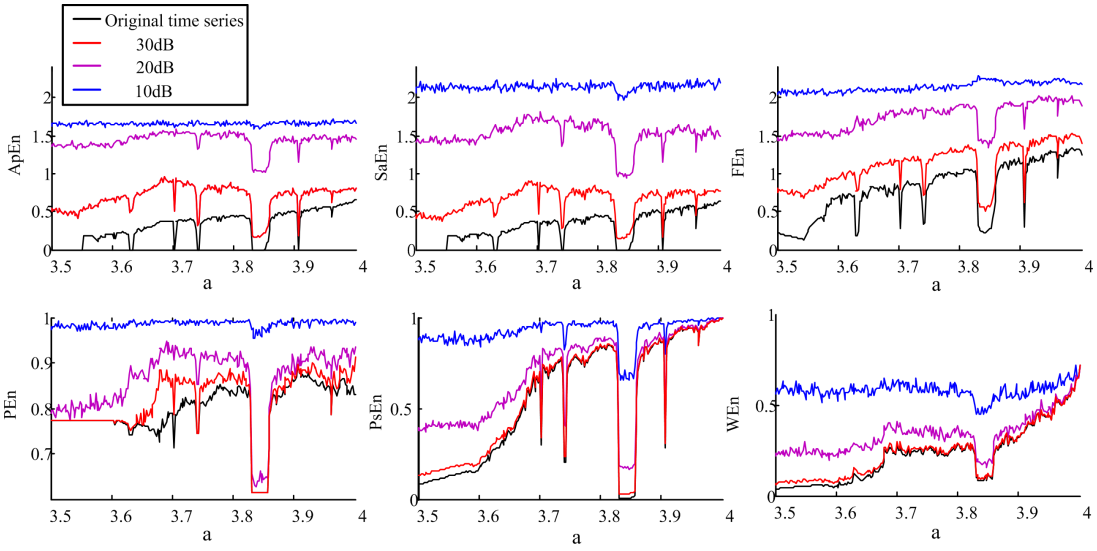

Fig. 2. The influence of noise levels (10, 20, 30 dB) on ApEn, SaEn, FEn, PEn, PsEn and WEn algorithms.

Table 2. Correlation coefficients between each entropy and the maximal Lyapunov exponent ($p < 0.01$).

	Original signal	SNR (30 dB)	SNR (20 dB)	SNR (10 dB)	Original signal	SNR (30 dB)	SNR (20 dB)	SNR (10 dB)
	ApEn				SaEn			
r1	0.9884	0.4574	0.3494	0.3513	0.9715	0.5260	0.4207	0.2488
r2	0.9892	0.5346	0.4012	0.4025	0.9804	0.5691	0.5138	0.3311
	FEn				PEn			
r1	0.9658	0.9646	0.9227	0.6666	0.7904	0.7917	0.6604	0.5299
r2	0.9661	0.9504	0.9248	0.6702	0.7976	0.7969	0.6880	0.5139
	PsEn				WEn			
r1	0.9494	0.9491	0.9392	0.8028	0.9210	0.9174	0.8781	0.4382
r2	0.9536	0.9530	0.9407	0.8101	0.9239	0.9148	0.8471	0.4686

Note: All entropies were significantly positive correlated to the positive maximal Lyapunov exponent ($p < 0.001$). The coefficient $r1$ indicates correlation between each entropy and the maximal Lyapunov exponent, and the coefficient $r2$ indicates correlation between each entropy based on EMD and the maximal Lyapunov exponent.

performance. With the increase of noise levels (SNR 10 dB), the correlation coefficient $r1$ of PsEn was highest. So, PsEn had the best anti-noise performance and PEn followed.

The correlation coefficients $r2$ between each entropy based on EMD and the maximal Lyapunov exponent increased compared to $r1$, which indicated that the entropies based on EMD had a better performance to analyze series complexity. Thus, the entropies based on EMD were used in the following analysis.

2.4.2. *The influence of series length on entropies algorithm*

The influence of the series length in the six algorithms is shown in Fig. 3. The system parameter a was 4, the time series length N varied from 100 to 2500 and its step size was 100.

In Fig. 3, the values of PsEn had a relatively stable fluctuation when the series length was greater than 500. The values of ApEn, SaEn and PEn had a relatively stable fluctuation when the series length

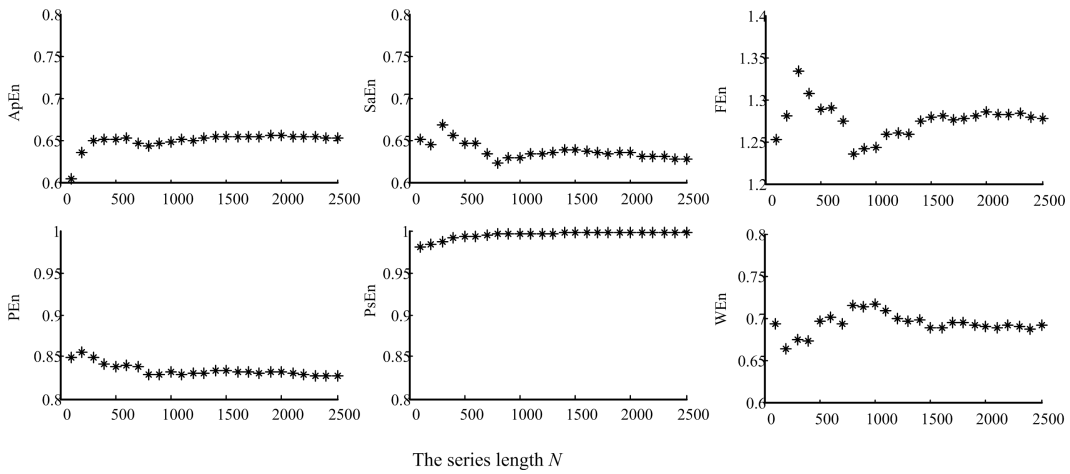

Fig. 3. The influence of different series length on ApEn, SaEn, FEn, PEn, PsEn and WEn algorithms.

was greater than 800, and the values of FEn and WEn had a relatively stable fluctuation when the series length was greater than 1500. So, PsEn has a real value with short data length, but FEn and WEn need more data.

2.5. *Statistical analysis and correlation analysis*

One way analysis of variance (ANOVA) was performed to test differences in six entropy measures between the aMCI and control group. The LSD test for *post-hoc* independent t-tests was used to compare each group difference separately in each electrode. Significant level was set at $p < 0.05$. Statistical analysis was carried out using SPSS 20.0 software (IBM SPSS Statistics Standard, Version 20.0).

Pearson's linear correlation was used to study the associations between entropy values and cognitive functions. Correlation coefficients between entropy values and neuropsychological tests were calculated in all patients (aMCI and control groups) as a single group. Significant level was set at $p < 0.01$.

2.6. *Salient feature selection and classification by SVMs*

These features were grouped into six feature sets: ApEn, SaEn, FEn, PEn, WEn and PsEn. Combined feature sets were also investigated to overcome the shortcomings of the extracted single feature. Hence, we will refer to the "All" feature set that combines all extracted features.

The most frequently used performance measure extracted from the receiver operating characteristics (ROC) curve is the value of the AUC, commonly denoted as AUC. Here, AUC curve was used to extract salient features from "All" feature set for the classification of aMCI patients and control group in T2DM. Once salient features were selected, the SVM-based classifier was explored. SVM is now well-founded and largely used in a number of applications, for example machine, images and diagnostics. Recent developments in defining and training statistical classifiers make it possible to build reliable classifiers in very small sample size problems. SVM has shown to work effectively in combination with kernels that map the data to other high-dimensional space by means of nonlinear transformations, where the data can be separated in a linear way, and establish the optimizing classification. In this paper, a polynomial kernel function with the default parameter values: regularization coefficient $C = 1$ and $\gamma = 0.01$ was used. 50% of the data was randomly set aside for feature selection. The remaining 50% was used for classifier training/testing using a cross validation. Classification accuracy, sensitivity and specificity were computed 50 times and given by their mean values.

3. Results

3.1. *Statistical analysis of entropies based on EMD between aMCI and control group*

Results of ANOVA are shown in Fig. 4. There were significant effects of group for the ApEn based on EMD ($F(1, 21) = 3.324$, $p < 0.001$), the SaEn based on EMD ($F(1, 21) = 3.662$, $p < 0.001$), the FEn

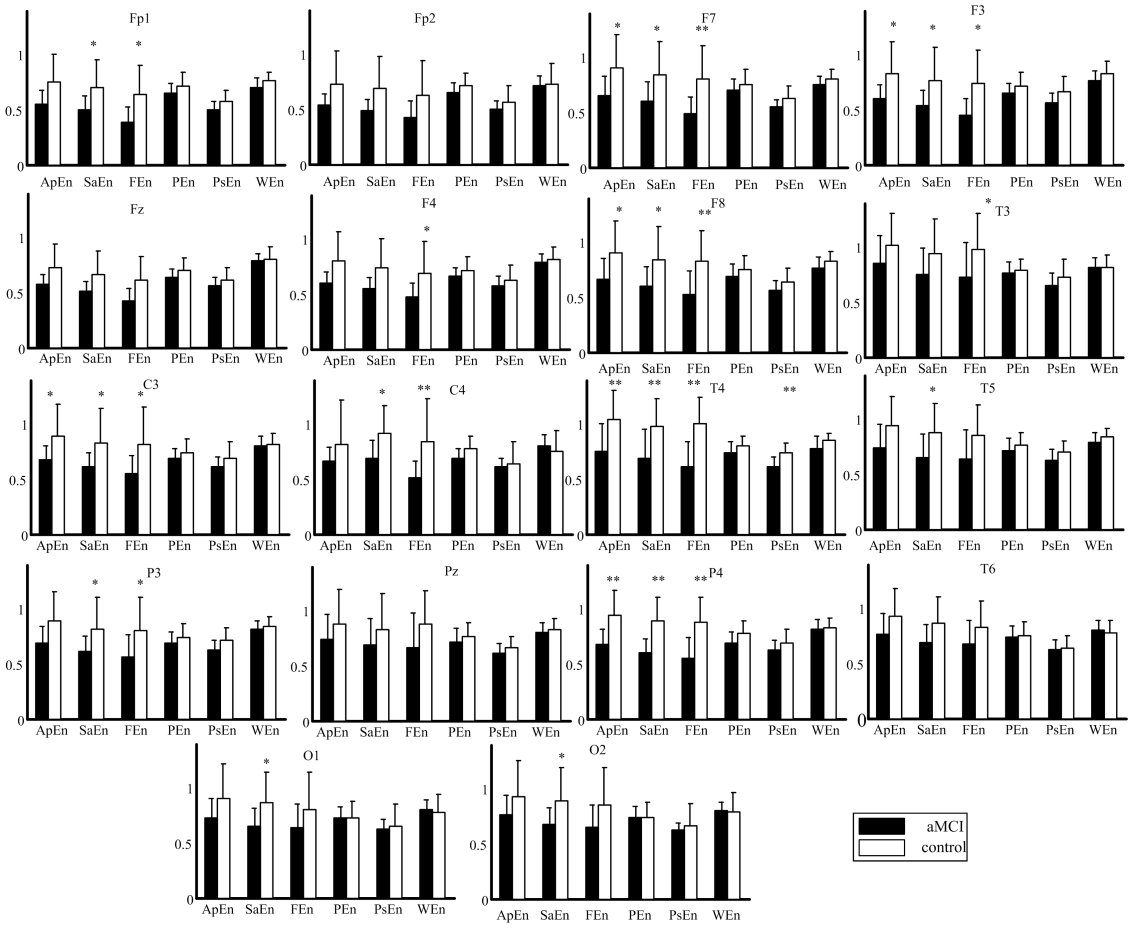

Fig. 4. The ApEn, SaEn, FEn, PEn, PsEn and WEn based on EMD at all electrodes (mean ± standard error) between aMCI group (black) and control group (white). Results of ANOVA were the following: there was the significant group effect for the ApEn based on EMD ($F(1, 21) = 3.324$, $p < 0.001$), the SaEn based on EMD ($F(1, 21) = 3.662$, $p < 0.001$), the FEn based on EMD ($F(1, 21) = 2.466$, $p < 0.001$) and the PsEn based on EMD ($F(1, 21) = 2.438$, $p < 0.001$); the PEn and WEn based on EMD group effects (($F(1, 21) = 1.396$, $p > 0.05$), $F(1, 21) = 1.164$, $p > 0.05$, respectively) were not significant. *Post-hoc* comparisons between aMCI and control group were illustrated on the top of the map: $^*p < 0.05$, $^{**}p < 0.01$.

based on EMD ($F(1, 21) = 4.366$, $p < 0.001$) and the PsEn based on EMD ($F(1, 21) = 2.438$, $p < 0.001$), But the PEn based on EMD and the WEn based on EMD group effects (($F(1, 21) = 1.396$, $p > 0.05$), $F(1, 21) = 1.164$, $p > 0.05$, respectively) were not significant. *Post-hoc* comparisons between aMCI and control group revealed that (1) aMCI group had lower ApEn based on EMD values compared with control group, with significant differences at electrodes F7, F3, F8, C3, T4 and P4 ($p < 0.036$ to $p < 0.005$); (2) aMCI group had lower SaEn based on EMD values compared with control group, with significant differences at electrodes Fp1, F7, F3, F8, C3, C4, T4, T5, P3, P4, O1 and O2 ($p < 0.044$ to $p < 0.004$); (3) aMCI group had lower FEn based on EMD values compared with control group, with significant differences at electrodes Fp1, F7, F3, F4, F8, T3, C3, C4, T4, P3 and P4 ($p < 0.005$ to $p < 0.003$); (4) aMCI group had lower PsEn based on EMD values compared with control group, with significant differences at electrodes T4 ($p < 0.01$); (5) aMCI group had lower WEn based on EMD values at almost all electrodes except C4, T6, O1 and O2, but the differences were not significant.

3.2. *Salient features extraction and classification of aMCI and control group*

Table 3 shows classifier accuracy, sensitivity and specificity for all features sets between the aMCI and control group. Accuracies of 65.7%, 65%, 68% and 63.1% were obtained with ApEn, SaEn, FEn

Table 3. Performance values of per feature set, Columns labeled "A, S and Sp" corresponding to accuracy, sensitivity and specificity, respectively.

A	S	Sp	A	S	Sp	A	S	Sp	A	S	Sp
ApEn			SaEn			FEn			PEn		
0.657	0.63	0.776	0.65	0.631	0.742	0.68	0.671	0.719	0.515	0.516	0.674
PsEn			WEn			All			All-43[a]		
0.56	0.543	0.601	0.524	0.259	0.348	0.631	0.61	0.734	0.738	0.723	0.779

Note: All-43 indicates the top 43 salient features of accuracy, sensitivity and specificity from the "All" feature set.

and "All" feature set, respectively, whereas accuracies of PEn, PsEn and WEn were relatively low.

Table 4 shows the top 43 salient features for the aMCI and control group, which were shifted from the "All" feature set. These features were represented by using an "electrode-feature" where "electrode" indicates the electrode positions (i.e., Fp1), and "feature" indicates six entropy feature sets (i.e., ApEn). In the table, SaEn, FEn and ApEn features were the most salient. When combined, they corresponded to 76.7% of the top 43 salient features selected. PSEn and PEn correspond to 16.3% and 7% of the top 43 salient features selected, respectively. However, WEn was seldom selected, so it plays a small role in aMCI detection.

In terms of brain region and electrode, features extracted from the right-temporal and occipital regions were highest ranking features, and P4, T4 and C4 were salient in top 10 electrodes and were shown in Fig. 5.

Table 4. Top 43 salient features selected by an AUC curve based feature selection algorithm.

Rank	Feature	Rank	Feature
1	P4-FEn	23	F7-PsEn
2	P4-SaEn	24	F8-ApEn
3	T4-FEn	25	P3-ApEn
4	T4-PSEn	26	Fp1-FEn
5	P4-ApEn	27	P4-PEn
6	C4-FEn	28	F8-ApEn
7	F7-FEn	29	Fz-ApEn
8	F8-FEn	30	T5-FEn
9	C4-SaEn	31	C3-PsEn
10	Fz-FEn	32	F3-PsEn
11	P3-FEn	33	F8-SaEn
12	T4-SaEn	34	O1-SaEn
13	F3-FEn	35	O2-SaEn
14	T4-ApEn	36	C4-ApEn
15	C3-FEn	37	F4-FEn
16	P3-PsEn	38	Fp2-FEn
17	T5-SaEn	39	T3-FEn
18	T6-SaEn	40	T4-PEn
19	F3-ApEn	41	Fp1-PsEn
20	F7-ApEn	42	F3-SaEn
21	T5-ApEn	43	P3-SaEn
22	C4-PEn		
Number of features per feature set			
ApEn	9	PEn	3
SaEn	10	PSEn	7
FEn	14	WEn	0
Number of features per brain region			
frontal	8		
central	8		
left-temporal	7		
right-temporal	10		
occipital	10		

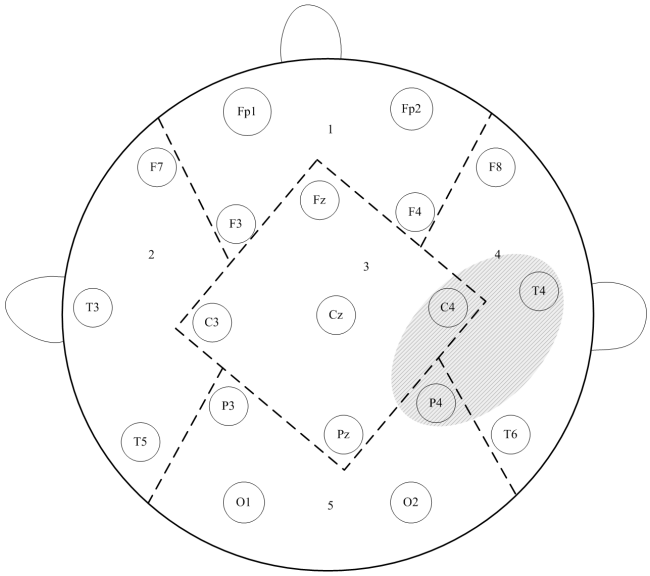

Fig. 5. Diagrammatic sketch of EEG zones. "1, 2, 3, 4 and 5" correspond to frontal, left-temporal central, right-temporal and occipital region, respectively. Gray scale indicated salient brain regions.

Table 5. Pearson's correlation analysis (r and p values) between each entropy and the scores of the neuropsychological tests in all subjects as a whole group ($p < 0.01$).

	FEn								
p_test	FP1	FP2	F7	F3	T4	P4	T5	O1	O2
MoCA					0.675	0.585			
					0.0008	0.005			
Semantic fluency							0.582	0.664	0.645
							0.006	0.001	0.002
AVLT immediate recall	0.594	0.587	0.714	0.596		0.685			0.583
	0.005	0.005	0.0002	0.004		0.0006			0.006
AVLT delay recall			0.660		0.596	0.726			
			0.001		0.004	0.0002			
	F8	P3	T6						
AVLT immediate recall	0.702	0.594							
	0.0004	0.005							
AVLT delay recall	0.635	0.555	0.561						
	0.002	0.009	0.008						
	PsEn								
p_test	F7	T3	C3	T4	P3	Pz	P4	O1	O2
MoCA				0.678					
				0.0007					
Semantic fluency								0.616	0.548
								0.003	0.005
AVLT immediate recall	0.582						0.571		
	0.0056						0.007		
AVLT delay re-evoke	0.597	0.571	0.562	0.658	0.582	0.605	0.560		
	0.0043	0.007	0.008	0.001	0.006	0.004	0.008		
	WEn								
p_test	F8								
Trail making B	−0.611								
	0.007								
	ApEn								
p_test	T4						P4		
MoCA							0.567		
							0.007		
AVLT delay recall				0.568					
				0.007					
	SaEn								
p_test	T4						P4		O2
MoCA							0.603		0.557
							0.004		0.009
AVLT delay recall				0.580			0.554		
				0.006			0.009		

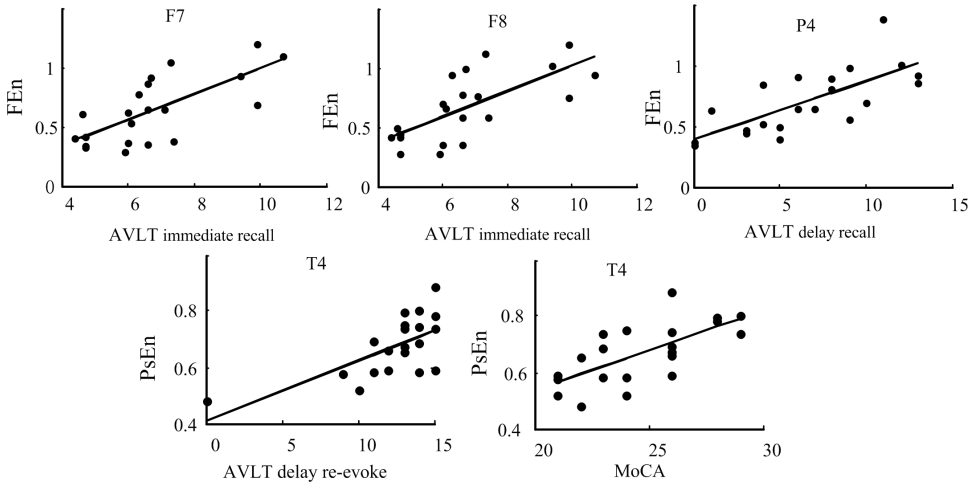

Fig. 6. Correlation results between neuropsychological tests and each entropy based on EMD for each electrode in all patients as a whole group (only significant correlations were displayed).

3.3. *Correlation analysis between entropies and cognitive functions*

In order to investigate the correlation between the cognitive functions and entropy based on EMD, the correlation coefficients between neuropsychological tests and each entropy at all electrodes were calculated using Pearson's linear correlation analysis between all patients as a whole group. The results are presented in Table 5 with correlation values r and p values ($p < 0.01$).

Then, Bonferroni method was used to correct the correlation in each entropy feature set. The results are shown in Fig. 6 (1) FEn based on EMD values were significantly positively correlated to the AVLT immediate recall at electrode F7 and F8 ($r = 0.714$, $p = 0.0003$, and $r = 0.702$, $p = 0.0004$, respectively) and delayed recall at electrode P4 ($r = 0.726$, $p = 0.0002$); (2) PsEn based on EMD values were significantly positively correlated to MoCA at electrodes T4 ($r = 0.678$, $p = 0.0007$) and AVLT delay re-evoke at electrode T4 ($r = 0.658$, $p = 0.001$). Thus, entropy based on EMD was significantly positively correlated to MoCA and memory.

4. Discussion

In this paper, six entropies based on EMD measures were employed to investigate the different dynamic characteristics between amnesic MCI and normal cognitive function subjects in T2DM. Compared to other entropies, FEn based on EMD had a higher classification accuracy. P4, T4 and C4 were highest ranking salient electrodes in top 43 salient features. FEn based on EMD was positively correlated to memory at electrodes F7, F8 and P4. So, FEn based on EMD in right-temporal and occipital regions may display better EEG characteristics correlated with cognitive functions and may be more suitable for distinguishing aMCI in T2DM.

Recently, several studies based on entropy have been successfully used to study the DM.[25,26] Molinari *et al.* showed that sample and bispectral entropy analysis could compare the inner structure of the near-infrared spectroscopy (NIRS) signals during muscle contraction, particularly when dealing with neuromuscular impairments.[27] Tarvainen *et al.* found that Diabetes duration was strongly associated with Renyi entropy which increased for positive orders and decreased for negative orders as a function of disease duration. Shannon entropy, SaEn and multiscale entropy (MSE) did not correlate with disease duration.[25] What is noteworthy is that each entropy method has its advantages. SaEn is independent of record length to reduce biases of ApEn, and has more accurate definition in theory compared with ApEn. Compared with ApEn and SaEn, FEn can obtain more detailed character of the time series and has more accurate definition in theory.[51] PEn is less sensitive to the signal quality and calculation length.[52] PsEn has the particular advantage that the contributions to entropy from any particular frequency range are explicitly separated.[53] Compared with PsEn, the window function

of WEn is variable in both the time and frequency domains. Which entropies are suitable for researching cognitive function in T2DM? To our knowledge, we firstly applied entropies based on EMD measures to analyze the dynamic characteristics in amnestic MCI with T2DM.

In simulation analysis, all entropies could effectively reflect the complexity and predictability of the chaotic series, except that PEn had a lower correlation coefficient of 0.7904. FEn had a good anti-noise performance, but longer data were needed. In the analysis of EEG data of patients in T2DM, results showed that maximum accuracy, sensitivity and specificity of 68%, 67.1% and 71.9% could be obtained with FEn. FEn may be the most suitable to distinguish characteristics between aMCI and control group in the six entropies. None of features extracted from the WEn feature set was selected, so WEn plays a small role in aMCI detection. Accuracy, sensitivity and specificity of 73.8%, 72.3% and 77.9% could be obtained with the top 43 salient features selected from "All" feature set, respectively, so the top 43 salient features selected compares favorably with single entropy and all entropy.

EMD is self-adaptive in nature and decomposes a signal on the basis of its frequency content and variation.[54] In recent years, EMD algorithm has become an established tool for the decomposition and time-frequency analysis of nonstationary signals.[55–57] It has been applied to various research fields such as mechanical and vibration, flow, speech, EEG, radar, earthquake or ocean, for revealing the underlying oscillatory modes of real-world signals.[58] The IMFs produced by the EMD method usually have physical meanings. Each IMF captures the properties of the original signal at different time scales and shifts them out in time domain, whereas each IMF respectively contains different frequency components from high to low in frequency domain. The IMFs extracted by the EMD method are more concentrated on main characteristics than original signal, so the use of EMD before computing entropy provides greater insight than simply applying the entropy measures to the whole signal. Tsai *et al.* have used EMD-based detrended SaEn to research the EEG in AD. Results showed that the SaEn calculated from the detrended EEG signals provides more sensitive results in early stage AD patients and provides an objective, noninvasive and nonexpensive tool for evaluating and following AD patients.[14]

Moreover, features extracted from the right-temporal and occipital regions were most salient at about 46.5%, which were similar with previous findings in the occipital region of AD but not diabetes patients.[17] We note that P4 was highly salient in these entropies. This is consistent with the facts that there was the decreased irregularity of the EEG with MCI and AD patients but not diabetes patients.[16,17,24] We also found that ApEn, SaEn and FEn entropy at electrodes F7, F3, F8, C3 and T4 had significantly decreased. It seems to be pathophysiologically meaningful, in that they may be related to cognitive impairment in T2DM.

Results of correlation analysis showed that the values of MoCA were correlated with the entropy based on EMD in right-temporal region but not MMSE. A number of studies have compared the sensitivity and specificity of two cognitive screening tools, namely MMSE and MoCA. Results showed that the MoCA score is more sensitive to detect the MCI and AD in comparison with MMSE.[59–61] In addition, the MoCA has comprehensive coverage of cognitive function, such as executive function attention, attention and delayed recall, while the MMSE lacks these abilities.[62] Recently, Alagiakrishnan *et al.* have compared the usefulness of MoCA with the Standardized MMSE in detecting MCI with T2DM. Results showed that MoCA may be more sensitive than the Standardized MMSE to detecting MCI in DM subjects. MoCA appears to be a better screening test than the Standardized MMSE for detecting MCI in middle-aged and elderly patients with T2DM.[63] In this study, we found that some entropy measures had significant correlation with MoCA, but were not significantly correlated with MMSE. The MoCA as a screening tool may be useful for providing quick guidance and for further investigation of MCI with T2DM. In addition, FEn based on EMD was significantly positively correlated with language and memory, PsEn based on EMD was significantly positively correlated with memory.

The mechanism for T2DM on the cognitive impairment was not clear at all. Some studies suggested that few factors may increase the risk of dementia and cognitive decline in DM, such as hypoglycemia, insulin therapy, duration of diabetes, angina pectoris, myocardial infarction, transient ischemic attack, atrophy in the region of hippocampus and amygdale.[3,31] In addition, comorbidity conditions associated with T2DM, including hyperinsulinemia

and hypertension, may contribute to vascular disease and neurodegeneration.[4] A recent report on MRI abnormalities and cognitive changes found substantial white matter lesions and subcortical atrophies in T2DM patients.[64] These results emphasized that abnormal EEG changes in persons with T2DM were also associated with cognitive impairment.

However, there are some limitations in the present study. The reliability and persuasion of the results were much affected because of lack of the comparison of AD or normal control group and the small quantity of the patients with T2DM. Therefore, further work was required to acquire more data not only in T2DM but also in normal control or AD patients.

At present, we researched the EEG background activity characteristics of T2DM on a single scale. It cannot account for features related to structure and organization on a single scale other than over multiple scales, so MSE method may be more effective to analyze characteristics of T2DM. Some studies analyzed the variation of EEG signal in AD patients by using MSE, and the results demonstrated that the AD patients had less complexity at smaller scales when compared with healthy control subjects.[15,22,65] Park *et al.* evaluated the complexity of the signal in MCI, AD and normal subjects. The results demonstrated that EEG data from MCI subjects showed nearly the same complexity and EEG data from severe AD patients and showed a loss of complexity in the multiple time scales when compared to EEG data from normal subjects.[66] Wu *et al.* analyzed atherosclerosis in the aged and diabetic, and found that MSE analysis of pulse wave velocity could better reflect the impact of age and blood sugar control.[26] In future studies, we may analyze MSE for distinguishing the aMCI diabetes patients from normal diabetes patients.

5. Conclusion

In this paper, we explored six entropy analysis measures to analyze characteristics of the EEG signals between amnesic MCI and non-MCI patients in T2DM. It was found that FEn had the best classification performance than other entropies with accuracy, sensitivity and specificity of 68%, 67.1% and 71.9%. In addition, FEn had more remarkable features, and the right-temporal and occipital regions also were very significant in top 43 salient features extracted from the "All" feature set, achieving accuracy, sensitivity and specificity of 73.8%, 72.3% and 77.9%. Cognitive functions and entropy had some significant correlations. Results showed that FEn based on EMD and memory at electrodes F7, F8 and P4 were significantly strictly correlated. PsEn based on EMD and MoCA at electrodes T4 and memory at electrode T4 were significantly strictly correlated.

Acknowledgments

This work was supported by National Natural Science Funds for Distinguished Young Scholar of China (61025019); National Natural Science Foundation of China (61102005, 61271142) and Natural Science Foundation of Hebei Province of China (F2014203132).

Appendix A. The EMD Algorithm

EMD can decompose the signal into different IMFs. Each IMF satisfies two basic conditions: (1) the number of extrema and the number of zero crossings must be the same or differ at most by one; (2) at any point, the mean value of the envelope defined by the local maxima and the envelope defined by the local minima is zero. The detailed EMD algorithm for the signal $y(t)$ can be calculated as follows:

(1) The extrema of the signal are identified as y_1. Cubic spline interpolation between, respectively, the local maxima e_m and the local minima e_l, determines the upper and the lower envelopes. The mean of the envelopes is subtracted from the signal $m_1 = (e_m + e_l)/2$;
(2) If the remainder fulfils the conditions of IMF, and differs from the previous one according to a specified mean squared error stopping criterion, it is retained. This IMF is then subtracted from the signal $c_1 = y_1 - m_1$. The process is repeated on the signal residue until only a trend remains from which no more IMF can be derived;
(3) At the end of the decomposition the original signal $y(t)$ is represented as follows:

$$y(t) = \sum_{i=1}^{n} C_i + r_n \tag{A.1}$$

where $y(t)$ is the original signal, n is the number of IMFs, r_n is the final residue.

Appendix B. The ApEn Algorithm

ApEn can be used to quantify the complexity or irregularity of a signal and describes the rate of producing new information. It is the negative average natural logarithm of the conditional probability that two vectors that are similar for m points remain similar at the next point. For the dominant analyzed series $x(i)$ of N length, the ApEn can be described as follows: this series is constructed $N - m + 1$ vectors $X(1), X(2), \ldots, X(N - m + 1)$, and expressed as

$$X(i) = \{x(i), x(i+1), \ldots, x(i+m-1)\}, \quad 1 \le i \le N - m + 1, \tag{B.1}$$

where m is the embedding dimension.

Calculate the distance between $X(i)$ and $X(j)$ by $d[X(i), X(j)]$, as the maximum absolute difference between their respective scalar components.

$$d[X(i), X(j)] = \max_{k=1,2,\ldots,m} (|x(i+k-1) - x(j+k-1)|) \tag{B.2}$$

For a given $X(i)$, count the number of $j(j = 1 \sim N - m + 1, j \neq i)$ so that the distance of two vectors $X(i)$ and $X(j)$ is smaller than r, denoted as N_i. Then we define for each i,

$$C_i^m(r) = (N - m + 1)^{-1} N_i, \quad i = 1, 2, \ldots, N - m + 1, \tag{B.3}$$

where $C_i^m(r)$ is the probability of a vector $X(i)$ being similar to a vector $X(j)$ within the tolerance r. Next, calculate the natural logarithm of each $C_i^m(r)$, and average it over i:

$$\phi^m(r) = (N - m + 1)^{-1} \sum_i \ln C_i^m(r) \tag{B.4}$$

Similarly, when the embedding dimension increase $m + 1$, the above process is repeated:

$$\phi^{m+1}(r) = (N - m)^{-1} \sum_{i=1}^{N-m+1} \ln C_i^m(r). \tag{B.5}$$

Finally, the patterns of length m and threshold r, is defined as:

$$\mathrm{ApEn}(m, r, N) = \phi^m(r) - \phi^{m+1}(r). \tag{B.6}$$

Appendix C. The SaEn Algorithm

SaEn is a refinement of ApEn, and is the negative logarithm of the conditional probability where two sequences similar to m points remain similar at the next point, where self-matching is not included in calculating the probability. For the dominant analyzed series $x(i)$ of N length, the SaEn is defined by following steps: this series are constructed $N - m$ vectors $X(1), X(2), \ldots, X(N - m + 1)$ and expressed as

$$X(i) = \{x(i), x(i+1), \ldots, x(i+m-1)\}, \quad 1 \le i \le N - m + 1, \tag{C.1}$$

where m is the embedding dimension.

Calculate the distance between $X(i)$ and $X(j)$ by $d[X(i), X(j)]$, as the maximum absolute difference between their respective scalar components, defined as

$$d[X(i), X(j)] = \max_{k=1,2,\ldots,m} (|x(i+k-1) - x(j+k-1)|) \tag{C.2}$$

For a given $X(i)$, count the number of $j(j = 1 \sim N - m, j \neq i)$ so that the distance of two vectors $X(i)$ and $X(j)$ is smaller than r, denoted as C_i. Then we define for each i,

$$C_i^m(r) = (N - m)^{-1} C_i, \quad i = 1, 2, \ldots, N - m \tag{C.3}$$

Next define $B^m(r)$:

$$B^m(r) = (N - m)^{-1} \sum_{i=1}^{N-m} C_i^m(r) \tag{C.4}$$

Similarly, when the embedding dimension increase $m + 1$, the above process is repeated:

$$A^m(r) = (N - m)^{-1} \sum_{i=1}^{N-m} C_i^{m+1}(r) \tag{C.5}$$

Finally, the SaEn is estimated by:

$$\mathrm{SaEn}(m, r, N) = -\ln[A^m(r)/B^m(r)] \tag{C.6}$$

Appendix D. The FEn Algorithm

FEn is the negative natural logarithm of the conditional probability that two vectors remain similar for the next +1 points. For the dominant analyzed series $x(i)$ of N length, vector sequences of m length are constructed as follows:

$$\{X_i^m = \{x(i), x(i+1), \ldots, x(i+m-1)\} - u0(i), \quad i = 1, \ldots, N - m + 1\}, \tag{D.1}$$

where X_i^m represents m consecutive x values, commencing with the ith points and generalized by removing a baseline: $u0(i) = m^{-1}\sum_{j=0}^{m-1} x(i+j)$.

For given X_i^m, calculated the similarity degree D_{ij}^m between X_i^m and its neighboring vector X_j^m through a fuzzy function $\mu(d_{ij}^m, n, r)$

$$D_{ij}^m(n,r) = \mu(d_{ij}^m, n, r) = \exp(-(d_{ij}^m)^n/r), \quad \text{(D.2)}$$

where d_{ij}^m is the maximum absolute difference of the corresponding scalar components of X_i^m and X_j^m, and the fuzzy function $\mu(d_{ij}^m, n, r)$ is the exponential function.

Then we define $\varphi^m(n,r)$ as:

$$\varphi^m(n,r) = (N-m)^{-1}\sum_{i=1}^{N-m}\left[(N-m-1)^{-1}\sum_{j=1,j\neq i}^{N-m} D_{ij}^m\right]. \quad \text{(D.3)}$$

Similarly, when m increases to $m+1$, the above process is repeated:

$$\varphi^{m+1}(n,r) = (N-m)^{-1}\sum_{i=1}^{N-m}\left[(N-m-1)^{-1}\sum_{j=1,j\neq i}^{N-m} D_{ij}^{m+1}\right]. \quad \text{(D.4)}$$

Finally, when the length of data sets N is finite, the FEn is estimated by:

$$\mathrm{FEn}(m,n,r,N) = \ln[\varphi^m(n,r) - \varphi^{m+1}(n,r)]. \quad \text{(D.5)}$$

Appendix E. The PEn Algorithm

PEn is an effective complexity measure for time series which is based upon the comparison of the ordinal sequence of neighboring values. For the dominant analyzed series $x(i)$ of N length, this series is constructed:

$$X_i = [x(i), x(i+L), \ldots, x(i+(m-1)L)], \quad i = 1, 2, \ldots, N-(m-1)L, \quad \text{(E.1)}$$

where m and L are embedding dimension and time delay, respectively. Then x is arranged in an increasing order:

$$[x(i+(j_1-1)L) \leq x(i+(j_2-1)L) \leq \cdots \leq x(i+(j_m-1)L)]. \quad \text{(E.2)}$$

There will be $m!$ possible patterns π. The same pattern is sorted a group, and the probability of the ith permutation occurring is calculated as $p_i, i = 1, 2, \ldots, m!$. The PEn is defined as

$$H = -\sum_{i=1}^{m!} p_i \log p_i. \quad \text{(E.3)}$$

Finally, the normalized entropy can be defined as:

$$\mathrm{PEn} = H/\ln(m!). \quad \text{(E.4)}$$

Appendix F. The WEn Algorithm

The wavelet is a smooth and quickly vanishing oscillating function with good localization in both frequency and time. WEn has physiological meaning, and can well measure the disorder level in the signal. For the dominant analyzed series $x(i)$ of N length, the wavelet energy $E_j^{(N_j)}$ at each scale j is defined as:

$$E_j^{N_j} = \sum_k |C_j(k)|^2, \quad \text{(F.1)}$$

where N_j is the window length within each level, the wavelet coefficients $C_j(k)$ can be interpreted as the local residual errors between successive signal approximations at scales j and $j+1$. In consequence, the total energy can be obtained by

$$E_{\mathrm{tot}} = \|T\|^2 = \sum_i \sum_k |C_j(k)|^2 = \sum_i E_j \quad \text{(F.2)}$$

Then the normalized values which represent the relative wavelet energy at each scale j and window length N_j:

$$p_j = \frac{E_j^{N_j}}{E_{\mathrm{tot}}} = \frac{\sum_k |C_j(k)|^2}{\sum_i \sum_k |C_j(k)|^2}. \quad \text{(F.3)}$$

According to the Shannon entropy, the WEn is defined between scales as follows:

$$\mathrm{WEn} = -\sum_j p_j \log p_j. \quad \text{(F.4)}$$

References

1. E. Ginter, V. Simko, "Type 2 diabetes mellitus, pandemic in 21st century," *Adv. Exp. Med. Biol.* **771**, 42–50 (2012).
2. J. A. Luchsinger, C. Reitz, B. Patel, M. X. Tang, J. J. Manly, R. Mayeux, "Relation of diabetes to mild

cognitive impairment," *Archiv. Neurol.* **64**(4), 570–575 (2007).
3. D. G. Bruce, W. A. Davis, G. P. Casey, S. E. Starkstein, R. M. Clarnette, O. P. Almeida, T. M. E. Davis, "Predictors of cognitive decline in older individuals with diabetes," *Diabetes Care* **31**(11), 2103–2107 (2008).
4. J. S. Saczynski, M. K. Jonsdottir, M. E. Garcia, P. V. Jonsson, R. Peila, G. Eiriksdottir, E. Olafsdottir, T. B. Harris, V. Gudnason, L. J. Launer, "Cognitive impairment: An increasingly important complication of type 2 diabetes," *Am. J. Epidemiol.* **168**(10), 1132–1139 (2008).
5. Y. W. Zhang, X. Zhang, J. Q. Zhang, C. Liu, Q. Y. Yuan, X. T. Yin, L. Q. Wei, J. G. Cui, R. Tao, P. Wei, J. Wang, "Gray matter volume abnormalities in type 2 diabetes mellitus with and without mild cognitive impairment," *Neurosci. Lett.* **562**, 1–6 (2014).
6. E. M. C. Schrijvers, J. C. M. Witteman, E. J. G. Sijbrands, A. Hofman, P. J. Koudstaal, M. M. B. Breteler, "Insulin metabolism and the risk of Alzheimer disease The Rotterdam study," *Neurology* **75**(22) 1982–1987 (2010).
7. R. O. Roberts, D. S. Knopman, Y. E. Geda, R. H. Cha, V. S. Pankratz, L. Baertlein, B. F. Boeve, E. G. Tangalos, R. J. Ivnik, M. M. Mielke, R. C. Petersen, "Association of diabetes with amnestic and nonamnestic mild cognitive impairment," *Alzheimers Dement.* **10**(1), 18–26 (2014).
8. T. Cukierman, H. C. Gerstein, J. D. Williamson, "Cognitive decline and dementia in diabetes-systematic overview of prospective observational studies," *Diabetologia* **48**(12), 2460–2469 (2005).
9. M. Elgendi, F. Vialatte, A. Cichocki, C. Latchoumane, J. Jeong, J. Dauwels, "Optimization of EEG frequency bands for improved diagnosis of Alzheimer disease," *2011 Annual Int. Conf. IEEE Engineering in Medicine and Biology Society*, pp. 6087–6091 (2011).
10. T. Gili, M. Cercignani, L. Serra, R. Perri, F. Giove, B. Maraviglia, C. Caltagirone, M. Bozzali, "Regional brain atrophy and functional disconnection across Alzheimer's disease evolution," *J. Neurol. Neurosurg. Ps* **82**(1), 58–66 (2011).
11. C. Babiloni, R. Ferri, G. Binetti, A. Cassarino, G. Dal Forno, M. Ercolani, F. Ferreri, G. B. Frisoni, B. Lanuzza, C. Miniussi, F. Nobili, G. Rodriguez, F. Rundo, C. J. Stam, T. Musha, F. Vecchio, P. M. Rossini, "Fronto-parietal coupling of brain rhythms in mild cognitive impairment: A multicentric EEG study," *Brain Res. Bull.* **69**(1), 63–73 (2006).
12. J. E. Skinner, D. N. Weiss, J. M. Anchin, Z. Turianikova, I. Tonhajzerova, J. Javorkova, K. Javorka, M. Baumert, M. Javorka, "Nonlinear PD2i heart rate complexity algorithm detects autonomic neuropathy in patients with type 1 diabetes mellitus," *Clin. Neurophysiol.* **122**(7), 1457–1462 (2011).
13. Y. Chen, T. D. Pham, "Sample entropy and regularity dimension in complexity analysis of cortical surface structure in early Alzheimer's disease and aging," *J. Neurosci. Methods* **215**(2), 210–217 (2013).
14. P. H. Tsai, C. Lin, J. Tsao, P. F. Lin, P. C. Wang, N. E. Huang, M. T. Lo, "Empirical mode decomposition based detrended sample entropy in electroencephalography for Alzheimer's disease," *J. Neurosci. Methods* **210**(2), 230–237 (2012).
15. T. Mizuno, T. Takahashi, R. Y. Cho, M. Kikuchi, T. Murata, K. Takahashi, Y. Wada, "Assessment of EEG dynamical complexity in Alzheimer's disease using multiscale entropy," *Clin. Neurophysiol.* **121**(9), 1438–1446 (2010).
16. D. Abasolo, J. Escudero, R. Hornero, C. Gomez, P. Espino, "Approximate entropy and auto mutual information analysis of the electroencephalogram in Alzheimer's disease patients," *Med. Biol. Eng. Comput.* **46**(10), 1019–1028 (2008).
17. D. Abásolo, R. Hornero, P. Espino, D. Alvarez, J. Poza, "Entropy analysis of the EEG background activity in Alzheimer's disease patients," *Physiol. Meas.* **27**(3), 241–253 (2006).
18. F. J. Hsiao, W. T. Chen, Y. J. Wang, S. H. Yan, Y. Y. Lin, "Altered source-based EEG coherence of resting-state sensorimotor network in early-stage Alzheimer's disease compared to mild cognitive impairment," *Neurosci. Lett.* **558**, 47–52 (2014).
19. D. Abasolo, R. Hornero, P. Espino, D. Alvarez, J. Poza, "Multiway array decomposition analysis of EEGs in Alzheimer's disease," *J. Neurosci. Methods* **207**(1), 41–50 (2012).
20. P. Ghorbanian, D. M. Devilbiss, A. J. Simon, A. Bernstein, T. Hess, H. Ashrafiuon, Discrete wavelet transform EEG features of Alzheimer's disease in activated states, *2012 Annual Int. Conf. IEEE Engineering in Medicine and Biology Society*, pp. 2937–2940 (2012).
21. F. J. Fraga, T. H. Falk, L. R. Trambaiolli, E. F. Oliveira, W. H. L. Pinaya, P. A. M. Kanda, R. Anghinah, "Towards an EEG-based biomarker for Alzheimer's disease: Improving amplitude modulation analysis features," *Int. Conf. Acoust. Speech*, pp. 1207–1211 (2013).
22. J. Escudero, D. Abasolo, R. Hornero, P. Espino, M. Lopez, "Analysis of electroencephalograms in Alzheimer's disease patients with multiscale entropy," *Physiol. Meas.* **27**(11), 1091–1106 (2006).
23. G. Emmanuelle, H. H. Anne, M. Guillaume, C. Mathieu, L. Georges, "Complexity quantification

of signals from the heart, the macrocirculation and the microcirculation through a multiscale entropy analysis," *Biomed. Signal Process.* **8**(4), 341–345 (2013).

24. D. Abasolo, R. Hornero, P. Espino, J. Poza, C. I. Sanchez, R. de la Rosa, "Analysis of regularity in the EEG background activity of Alzheimer's disease patients with approximate entropy," *Clin. Neurophysiol.* **116**(8), 1826–1834 (2005).
25. M. P. Tarvainen, D. J. Cornforth, P. Kuoppa, J. A. Lipponen, H. F. Jelinek, Complexity of heart rate variability in type 2 diabetes — effect of hyperglycemia, *2013 Annual Int. Conf. IEEE Engineering in Medicine and Biology Society*, pp. 5558–5561 (2013).
26. H. T. Wu, P. C. Hsu, C. F. Lin, H. J. Wang, C. K. Sun, A. B. Liu, M. T. Lo, C. J. Tang, "Multiscale entropy analysis of pulse wave velocity for assessing atherosclerosis in the aged and diabetic," *IEEE Trans. Biomed. Eng.* **58**(10), 2978–2981 (2011).
27. F. Molinari, U. R. Acharya, R. J. Martis, R. De Luca, G. Petraroli, W. Liboni, "Entropy analysis of muscular near-infrared spectroscopy (NIRS) signals during exercise programme of type 2 diabetic patients: Quantitative assessment of muscle metabolic pattern," *Comput. Methods Prog. Biol.* **112**(3), 518–528 (2013).
28. M. A. H. Hazari, B. Ram Reddy, N. Uzma, B. S. Kumar, "Cognitive impairment in type 2 diabetes mellitus," *Int. J. Diabetes Mellitus* **01**, 1–6 (2011).
29. T. Brismar, "The human EEG-physiological and clinical studies," *Physiol. Behav.* **92**(1–2), 141–147 (2007).
30. G. K. Cooray, L. Maurex, T. Brismar, "Cognitive impairment correlates to low auditory event-related potential amplitudes in type 1 diabetes," *Psychoneuroendocrinology* **33**(7), 942–950 (2008).
31. G. K. Cooray, L. Hyllienmark, T. Brismar, "Decreased cortical connectivity and information flow in type 1 diabetes," *Clin. Neurophysiol.* **122**(10), 1943–1950 (2011).
32. N. E. Huang, Z. Shen, S. R. Long, M. C. Wu, H. H. Shih, Q. Zheng, N. C. Yen, C. C. Tung, H. Liu, "The empirical mode decomposition and the Hilbert spectrum for nonlinear and non-stationary time series analysis," *Phys. Eng. Sci.* **454**(1971), 903–995 (1998).
33. G. Puavilai, S. Chanprasertyotin, A. Sriphrapradaeng, "Diagnostic criteria for diabetes mellitus and other categories of glucose intolerance: 1997 criteria by the Expert Committee on the Diagnosis and Classification of Diabetes Mellitus (ADA), 1998 WHO consultation criteria, and 1985 WHO criteria. World Health Organization," *Diabetes Res. Clin. Pract.* **44**(1), 21–26 (1999).
34. F. Portet, P. J. Ousset, P. J. Visser, G. B. Frisoni, F. Nobili, P. Scheltens, B. Vellas, J. Touchon. "Mild cognitive impairment (MCI) in medical practice: A critical review of the concept and new diagnostic procedure. Report of the MCI Working Group of the European Consortium on Alzheimer's Disease," *J. Neurol. Neurosurg. Psychiatry* **77**(6), 714–718 (2006).
35. G. A. Carlesimo, C. Caltagirone, G. Gainotti, "The mental deterioration battery: Normative data, diagnostic reliability and qualitative analyses of cognitive impairment. The Group for the Standardization of the Mental Deterioration Battery," *Eur. Neurol.* **36**(6), 378–384 (1996).
36. G. Novelli, Three clinical tests for the assessment of lexical retrieval and production. Norms from 320 normal subjects, Archivio di psicologia, *Neurologia E Psichiatria* **47**, 477–506 (1986).
37. A. Orsini, D. Grossi, E. Capitani, M. Laiacona, C. Papagno, G. Vallar, "Verbal and spatial immediate memory span: Normative data from 1355 adults and 1112 children," *Ital. J. Neurol. Sci.* **8**(6) 539–548 (1987).
38. Reitan, "Validity of the trail making test as an indication of organic brain damage," *Percept. Mot. Skills* **958**, 271–276 (1958).
39. M. P. Lawton, E. M. Brody, "Assessment of older people: Self-maintaining and instrumental activities of daily living," *Gerontologist* **9**(3), 179–186 (1969).
40. S. M. Pincus, "Approximate entropy as a measure of system complexity," *Proc. Natl. Acad. Sci. USA* **88**, 2297–2301 (1991).
41. L. Guo, D. Rivero, A. Pazos, "Epileptic seizure detection using multiwavelet transform based approximate entropy and artificial neural networks," *J. Neurosci. Methods* **193**(1), 156–163 (2010).
42. M. G. Signorini, G. Magenes, S. Cerutti, D. Arduini, "Linear and nonlinear parameters for the analysis of fetal heart rate signal from cardiotocographic recordings," *IEEE Trans. Biomed. Eng.* **50**(3), 365–374 (2003).
43. S. M. Pincus, "Assessing serial irregularity and its implications for health," *Popul. Health Aging* **954**, 245–267 (2001).
44. J. Bruhn, H. Ropcke, A. Hoeft, "Approximate entropy as an electroencephalographic measure of anesthetic drug effect during desflurane anesthesia," *Anesthesiology* **92**(3), 715–726 (2000).
45. C. E. Elger, G. Widman, R. Andrzejak, M. Dumpelmann, J. Arnhold, P. Grassberger, K. Lehnertz, "Value of nonlinear time series analysis of the EEG in neocortical epilepsies," *Adv. Neurol.* **84**, 317–330 (2000).
46. L. Zadeh, Fuzzy sets, *Inform. Control* **8**(3), 338–353 (1965).

47. C. Bandt, B. Pompe, "Permutation entropy: A natural complexity measure for time series," *Phys. Rev. Lett.* **88**(17), 174102 (2002).
48. X. Li, G. Ouyang, D. A. Richards, "Predictability analysis of absence seizures with permutation entropy," *Epilepsy Res.* **77**(1), 70–74 (2007).
49. E. Olofsen, J. W. Sleigh, A. Dahan, "Permutation entropy of the electroencephalogram: A measure of anaesthetic drug effect," *Br. J. Anaesthesiol* **101**(6), 810–821 (2008).
50. J. W. Sleigh, D. A. Steyn-Ross, M. L. Steyn-Ross, C. Grant, G. Ludbrook, "Cortical entropy changes with general anaesthesia: Theory and experiment," *Physiol. Meas.* **25**(4), 921–934 (2004).
51. W. T. Chen, J. Zhuang, W. X. Yu, Z. Z. Wang, "Measuring complexity using FuzzyEn, ApEn, and SampEn," *Med. Eng. Phys.* **31**(1), 61–68 (2009).
52. X. L. Li, S. Y. Cui, L. J. Voss, "Using permutation entropy to measure the electroencephalographic effects of sevoflurane," *Anesthesiology* **109**(3), 448–456 (2008).
53. H. Viertiö-Oja, V. Maja, M. Särkelä, P. Talja, N. Tenkanen, H. Tolvanen-Laakso, M. Paloheimo, A. Vakkuri, A. Yli-Hankala, P. Meriläinen, "Description of the Entropy™ algorithm as applied in the Datex-Ohmeda S/5™ entropy module," *Acta Anaesthesiol. Scand.* **48**(2), 154–161 (2004).
54. Z. K. Peng, P. W. Tse, F. L. Chu, "A comparison study of improved Hilbert–Huang transform and wavelet transform: Application to fault diagnosis for rolling bearing," *Mech. Syst. Signal Process.* **19**(5), 974–988 (2005).
55. X. Y. Zhang, J. Z. Zhou, "Multi-fault diagnosis for rolling element bearings based on ensemble empirical mode decomposition and optimized support vector machines," *Mech. Syst. Signal Process.* **41**(1–2), 127–140 (2013).
56. J. R. Huang, S. Z. Fan, M. F. Abbod, K. K. Jen, J. F. Wu, J. S. Shieh, "Application of multivariate empirical mode decomposition and sample entropy in EEG signals via artificial neural networks for interpreting depth of anesthesia," *Entropy* **15**(9), 3325–3339 (2013).
57. X. Li, D. Li, Z. Liang, L. J. Voss, J. W. Sleigh, "Analysis of depth of anesthesia with Hilbert–Huang spectral entropy," *Clin. Neurophysiol.* **119** (11), 2465–2475 (2008).
58. A. Gallix, J. M. Gorriz, J. Ramirez, I. A. Illan, E. W. Lang, "On the empirical mode decomposition applied to the analysis of brain SPECT images," *Expert Syst. Appl.* **39**(18), 13451–13461 (2012).
59. C. Zadikoff, S. H. Fox, D. F. Tang-Wai, T. Thomsen, R. M. A. de Bie, P. Wadia, J. Miyasaki, S. Duff-Canning, A. E. Lang, C. Marras, "A comparison of the mini mental state exam to the Montreal cognitive assessment in identifying cognitive deficits in Parkinson's disease," *Mov. Disord.* **23**(2), 297–299 (2008).
60. D. R. Roalf, P. J. Moberg, S. X. Xie, D. A. Wolk, S. T. Moelter, S. E. Arnold, "Comparative accuracies of two common screening instruments for classification of Alzheimer's disease, mild cognitive impairment, and healthy aging," *Alzheimers Dement.* **9**(5), 529–537 (2013).
61. P. Athilingam, K. B. King, S. W. Burgin, M. Ackerman, L. A. Cushman, L. Chen, "Montreal cognitive assessment and mini-mental status examination compared as cognitive screening tools in heart failure," *Heart Lung* **40**(6), 521–529 (2011).
62. S. Nazem, A. D. Siderowf, J. E. Duda, T. T. Have, A. Colcher, S. S. Horn, P. J. Moberg, J. R. Wilkinson, H. I. Hurtig, M. B. Stern, D. Weintraub, "Montreal cognitive assessment performance in patients with Parkinson's disease with 'normal' global cognition according to mini-mental state examination score," *J. Am. Geriatr. Soc.* **57**(2), 304–308 (2009).
63. K. Alagiakrishnan, N. Zhao, L. Mereu, P. Senior, A. Senthilselvan, Montreal cognitive assessment is superior to standardized mini-mental status exam in detecting mild cognitive impairment in the middle-aged and elderly patients with type 2 diabetes mellitus, *Biomed. Res. Int.* 5 (2013), doi: 10.1155/2013/186106.
64. S. M. Manschot, A. M. A. Brands, J. van der Grond, R. P. C. Kessels, A. Algra, L. J. Kappelle, G. J. Biessels, U. D. E. St, "Brain magnetic resonance imaging correlates of impaired cognition in patients with type 2 diabetes," *Diabetes* **55**(4), 1106–1113 (2006).
65. A. C. Yang, S. J. Wang, K. L. Lai, C. F. Tsai, C. H. Yang, J. P. Hwang, M. T. Lo, N. E. Huang, C. K. Peng, J. L. Fuh, "Cognitive and neuropsychiatric correlates of EEG dynamic complexity in patients with Alzheimer's disease," *Prog. Neuropsychopharmacol Biol Psychiatry* **47**, 52–61 (2013).
66. J. H. Park, S. Kim, C. H. Kim, A. Cichocki, K. Kim, "Multiscale entropy analysis of EEG from patients under different pathological conditions," *Fractals* **15**(4), 399–404 (2007).